
Figures and figure supplements

Bovine F_1F_o ATP synthase monomers bend the lipid bilayer in 2D membrane crystals

Chimari Jiko, et al.

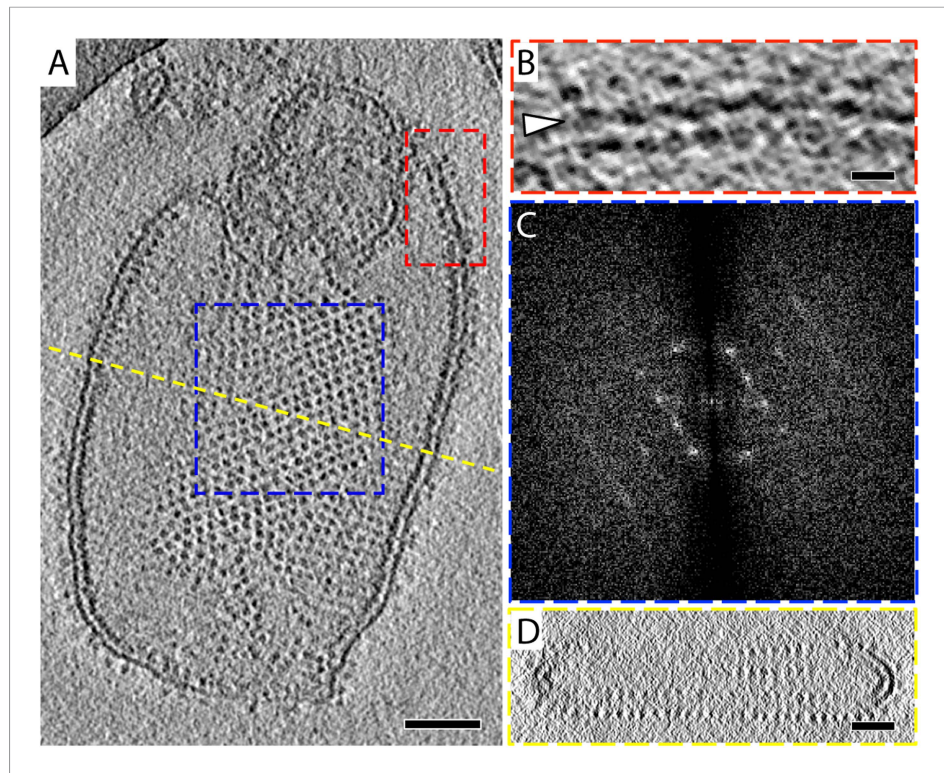


Figure 1. 2D crystals of F_1F_0 ATP synthase in vitreous ice. **(A)** Tomographic slice of a vesicle reconstituted with F_1F_0 ATP synthase. The ATP synthases appear as 10 nm spherical densities located 15 nm above the membrane. **(B)** Enlarged view of red boxed area in **(A)** showing the zigzag membrane structure (arrowhead). (See also **Figure 2**.) **(C)** Fourier transform of the blue-boxed area in **(A)**. **(D)** Cross-section along the yellow dashed line in **(A)**. Scale bar: **(A)** 100 nm, **(B)** 20 nm, **(D)** 50 nm.

DOI: [10.7554/eLife.06119.003](https://doi.org/10.7554/eLife.06119.003)

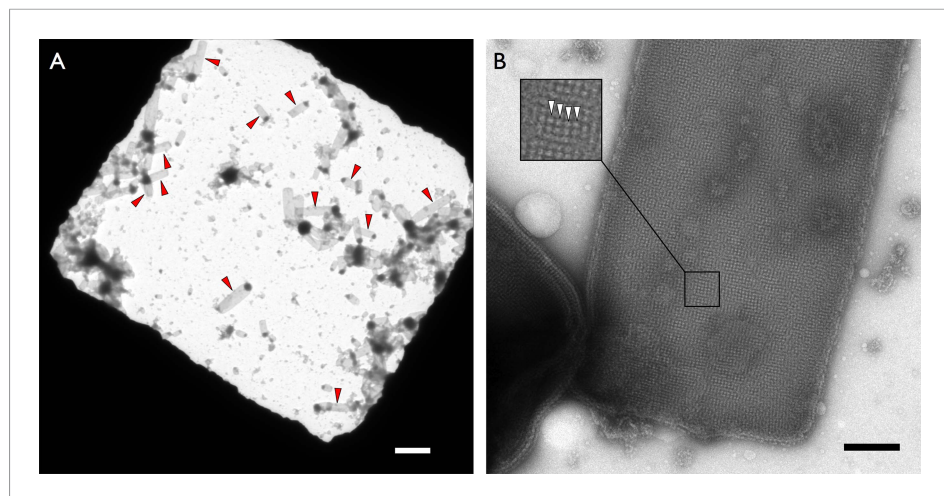


Figure 1—figure supplement 1. Crystalline vesicles of F_1F_0 ATP synthase in negative stain. **(A)** Overview of an EM grid square with numerous rectangular crystalline vesicles (red arrowheads). Scale bar 3 μm . **(B)** Rectangular crystalline vesicle at higher magnification with boxed area enlarged. F_1 heads (white arrowheads). Scale bar 200 nm.

DOI: [10.7554/eLife.06119.004](https://doi.org/10.7554/eLife.06119.004)

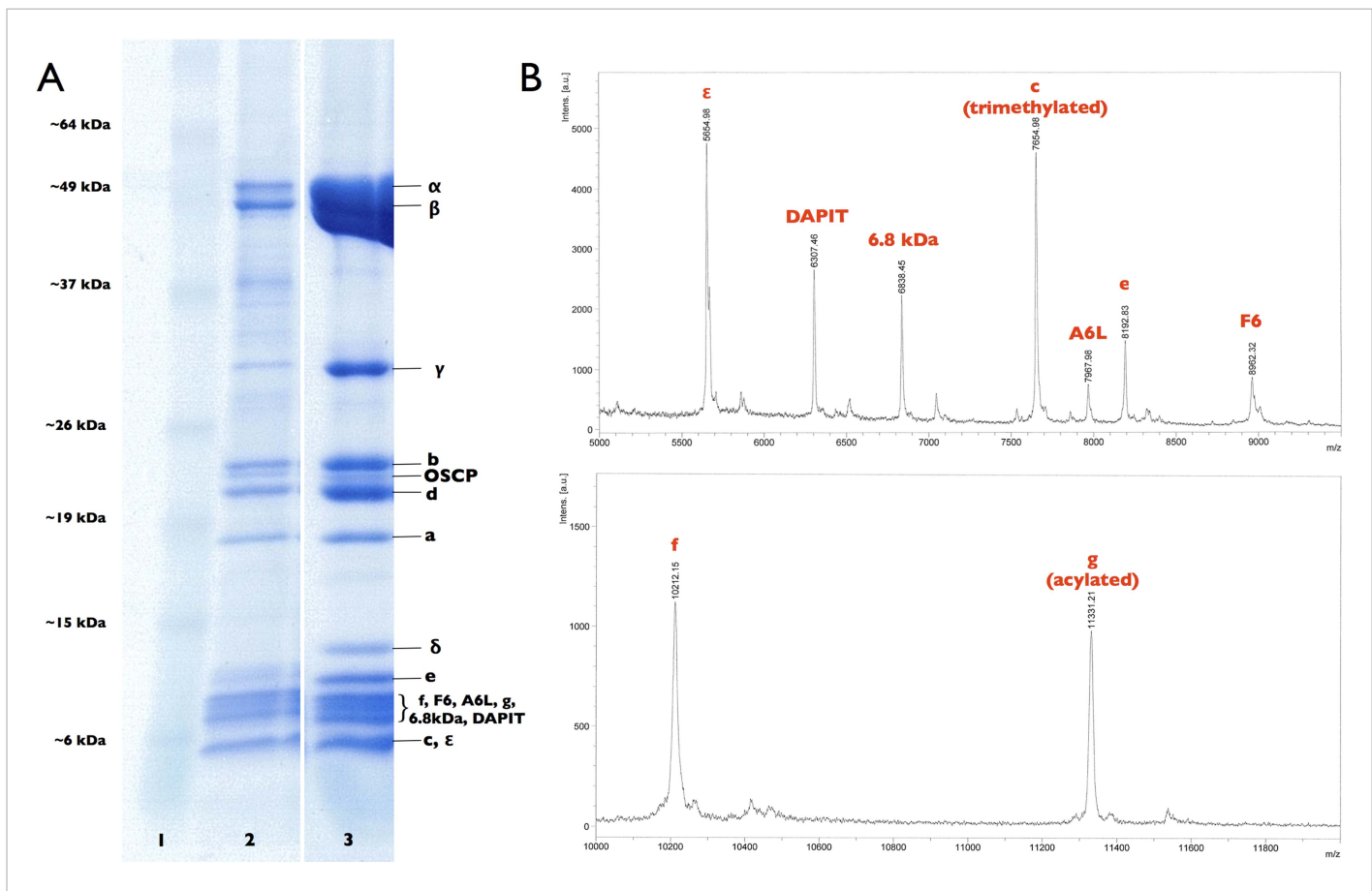


Figure 1—figure supplement 2. Subunit composition of F_1F_o ATP synthase isolated from 2D crystals. **(A)** SDS-polyacrylamide gradient gel (10–20%) showing the subunit composition of purified F_1F_o ATP synthases before (lane 2) and after (lane 3) 2D crystallisation. Lane 1, molecular marker (BenchMark). **(B)** Mass spectrometry profile of small subunits (5000–12,000 Da) of the F_1F_o ATP synthase isolated from 2D crystals. All F_1F_o ATP synthase subunits are present in the 2D crystals.

DOI: [10.7554/eLife.06119.005](https://doi.org/10.7554/eLife.06119.005)

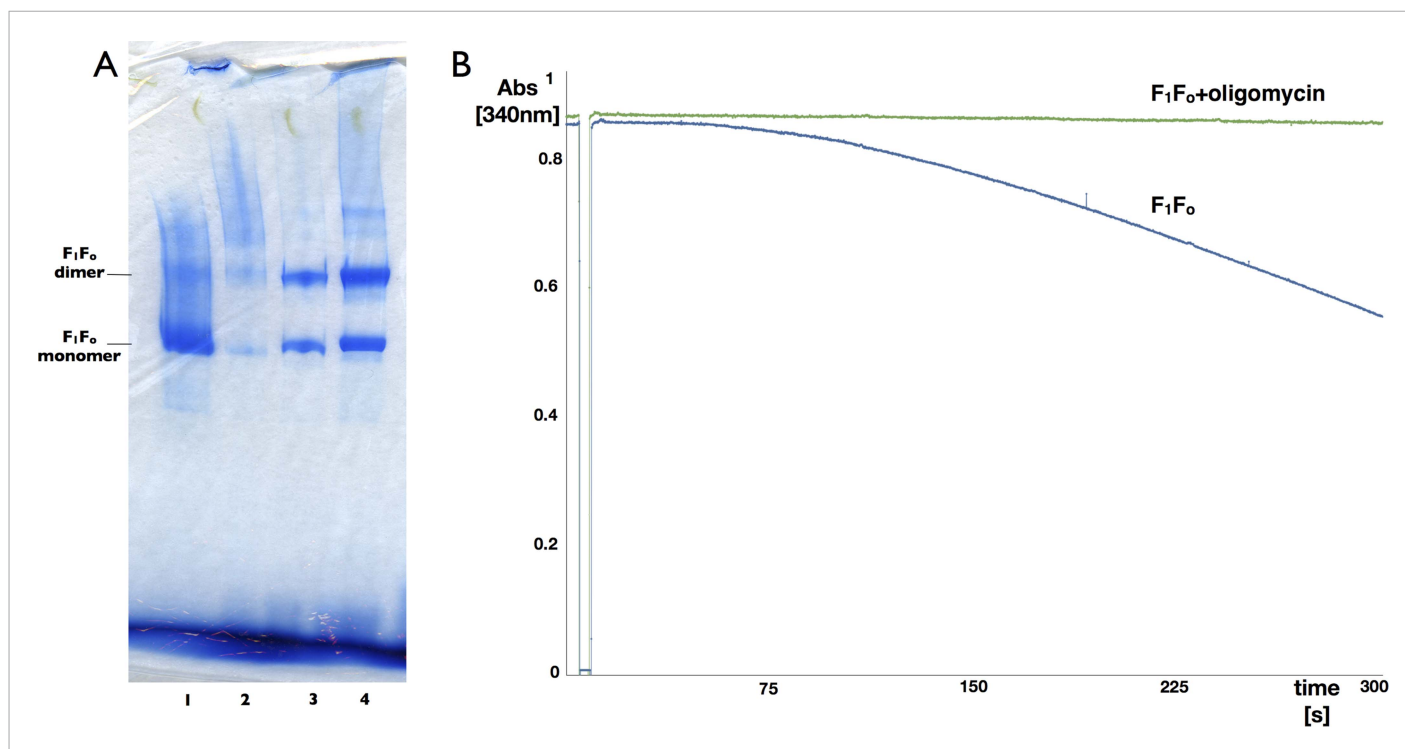


Figure 1—figure supplement 3. Blue-native polyacrylamide gel and activity assay of F_1F_0 ATP synthase isolated from 2D crystals. **(A)** BN polyacrylamide gradient gel (4–12%) of purified F_1F_0 ATP synthase solubilized in decylmaltoside (lane 1 and 2, 15 μ g and 2 μ g respectively) and of digitonin-resolubilised 2D crystals (lane 3 and 4, 30 μ g and 90 μ g respectively). Bands of lower molecular weight subcomplexes, that is, F_0 or c_8 , are weak or absent. The dimer band in lane 1 and 2 presumably stems from mitochondrial F_1F_0 ATP synthase dimers preserved by mild purification conditions. The dimer band visible in lane 3 and 4 most likely represents non-physiological F_1F_0 ATP synthase dimers that form in the 2D crystals. **(B)** Typical ATPase activity and oligomycin-sensitivity of digitonin-resolubilised F_1F_0 ATP synthase isolated from 2D crystals. The hydrolysis of ATP by the F_1F_0 ATP synthase was monitored using an enzyme couple assay by detecting NADH oxidation at 340 nm at 20°C in the absence (blue) or presence (green) of oligomycin. Oligomycin inhibits ATP hydrolysis through F_1 by stopping rotation of the F_0 motor, that is, oligomycin sensitivity gives a measure of the amount of coupled, intact F_1F_0 ATP synthase complexes in the preparation, in this case >95%.

DOI: [10.7554/eLife.06119.006](https://doi.org/10.7554/eLife.06119.006)

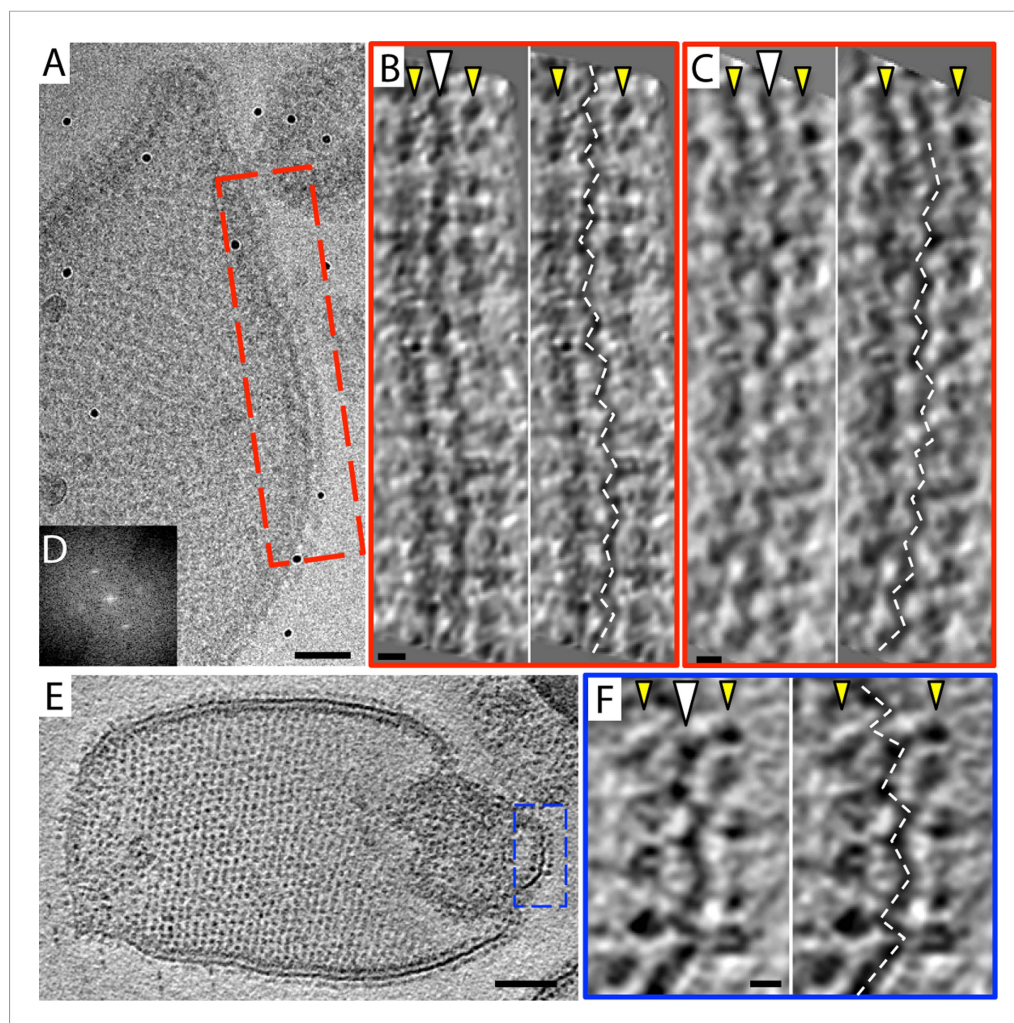


Figure 2. Zigzag membrane structure. (A) Projection image of a vesicle reconstituted with F_1F_o ATP synthase. (B) and (C) tomographic slices of boxed area in (A) at different z-heights. (D) Fourier transform of an oblique tomographic slice through boxed area in (A) showing weak diffraction. (E) Tomographic slice of rectangular crystalline vesicle. (F) Close-up of boxed area in (E). White arrowhead, indicates membrane plane, yellow arrowhead, line of F_1 head groups. Scale bar: (A) 50 nm, (B, C, and F) 10 nm, (E) 100 nm.

DOI: [10.7554/eLife.06119.007](https://doi.org/10.7554/eLife.06119.007)

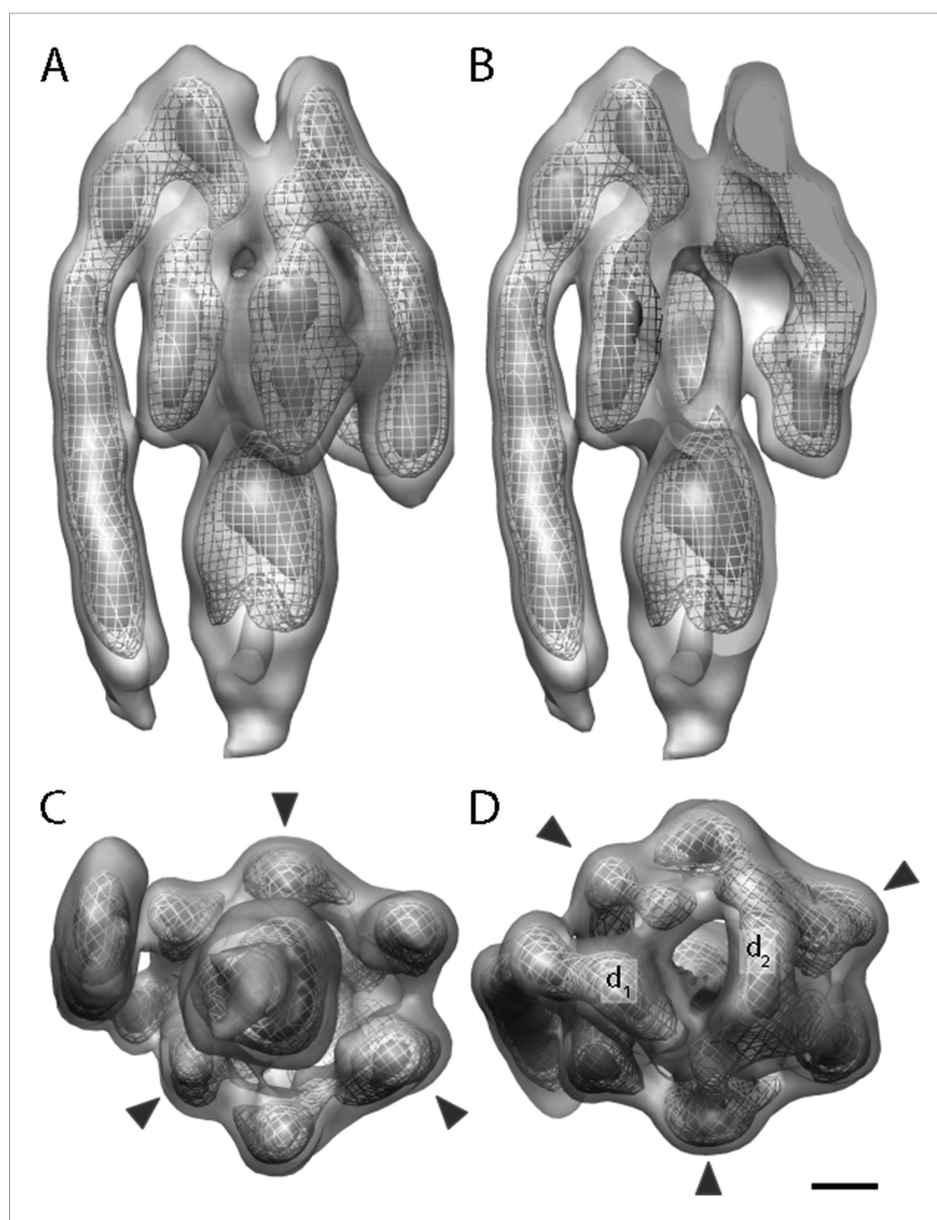


Figure 3. Sub-tomogram average of bovine heart mitochondrial F_1F_0 ATP synthase calculated from 2D crystals. (A) Surface view, (B) longitudinal section showing central stalk, (C) bottom view and (D) top view. Arrowheads: positions of the β subunits. d_1 and d_2 : densities connecting peripheral stalk to F_1 subcomplex. Threshold levels: light grey, 1 σ ; mesh, 3 σ ; dark grey, 5 σ . Scale bar: 20 Å.

DOI: [10.7554/eLife.06119.008](https://doi.org/10.7554/eLife.06119.008)

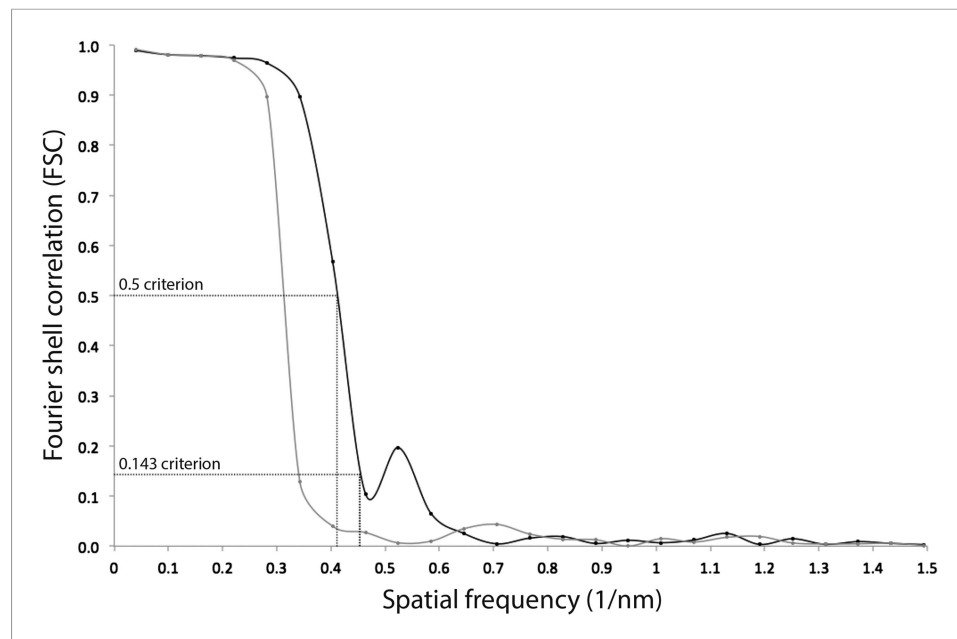


Figure 3—figure supplement 1. Resolution estimate of the ATP synthase monomer sub-tomogram average. Fourier shell correlation (FSC) curves were calculated by comparing averages generated from two independently processed data sets ('Gold standard'; *Scheres and Chen, 2012*, black line). To check for overfitting, phases beyond 40 Å were randomized (*Chen et al., 2013*) and the final alignment iteration repeated (grey line). According to the FSC 0.5 criterion (crosshairs), the ATP synthase monomer average has a resolution of 2.4 nm. Points on the FSC curves mark spatial frequency shells used in the FSC calculation.

DOI: [10.7554/eLife.06119.009](https://doi.org/10.7554/eLife.06119.009)

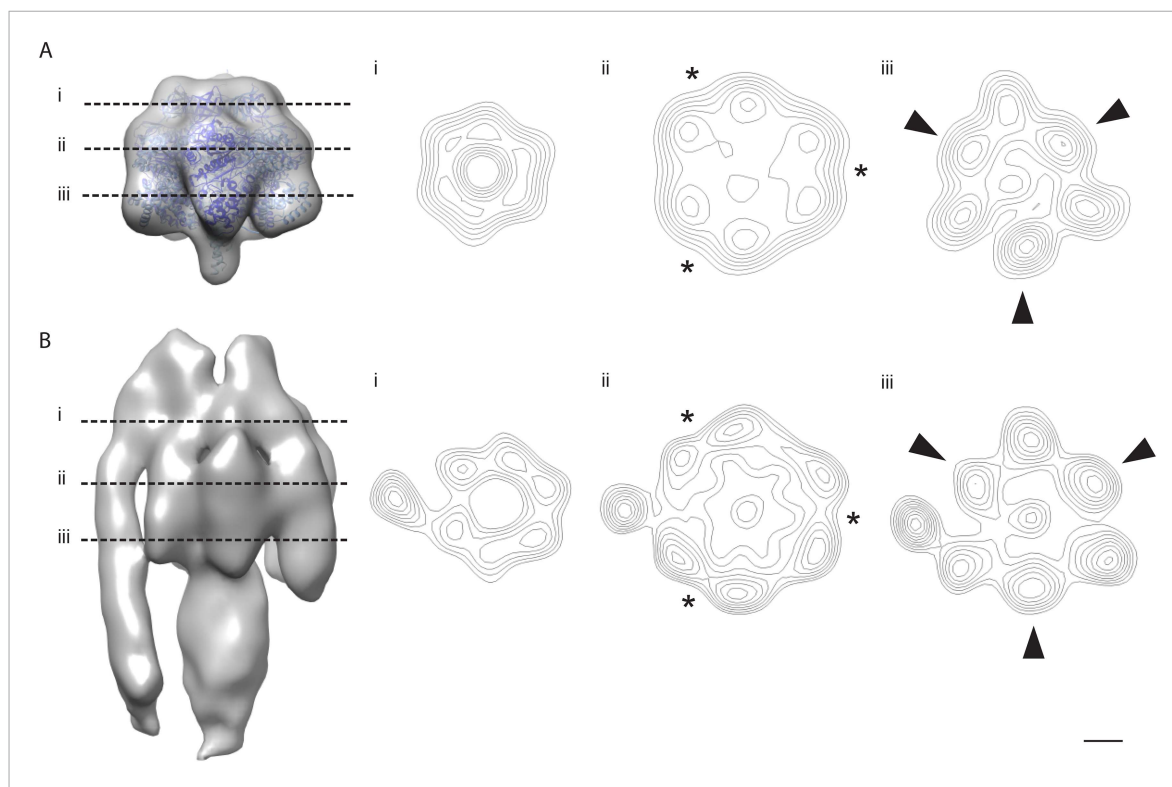


Figure 3—figure supplement 2. The α/β hexamer. **(A)** X-ray map of catalytic domain (PDB code: 1BMF, **Abrahams et al., 1994**) Fourier-filtered to 25 Å. **(B)** Subtomogram average calculated from 2D crystals. Dashed lines, cross-section levels in i–iii. Arrowheads, beta subunits *, catalytic interface between α and β subunits. Contour levels drawn at intervals of 0.5 sigma above mean. Scale bar, 20 Å.

DOI: [10.7554/eLife.06119.010](https://doi.org/10.7554/eLife.06119.010)

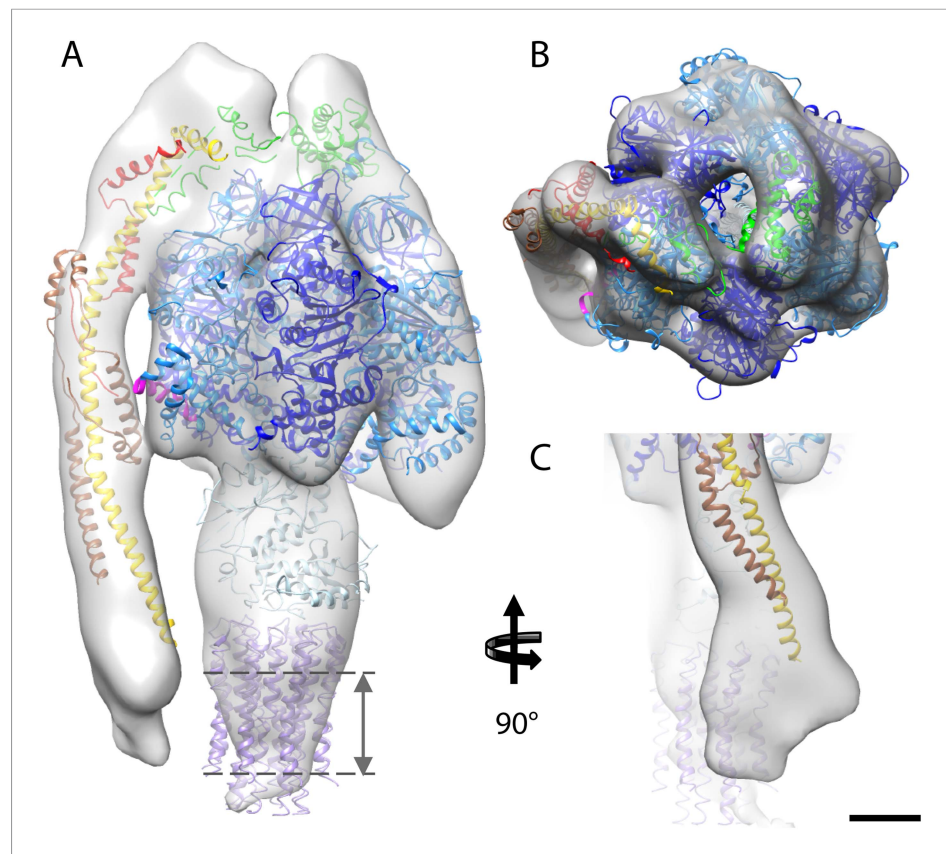


Figure 4. Fitted atomic model of the bovine F_1F_o ATP synthase. (A–C) Sub-tomogram average with fitted atomic models (A) side view, (B) top view, and (C) the peripheral stalk. Blue, catalytic domain; grey, central stalk; green, oligomycin sensitivity conferral protein (OSCP) from PDB:2WSS (Rees et al., 2009). Purple, c-ring (PDB:2XND) (Watt et al., 2010); Yellow-red, peripheral stalk fragment (PDB: 2CLY) (Dickson et al., 2006) with additional residues from PDB:2WSS (Rees et al., 2009). Pink, α -subunit helix thought to interact with the peripheral stalk. Dashed lines, position of membrane. Scale bar, 20 Å.

DOI: [10.7554/eLife.06119.011](https://doi.org/10.7554/eLife.06119.011)

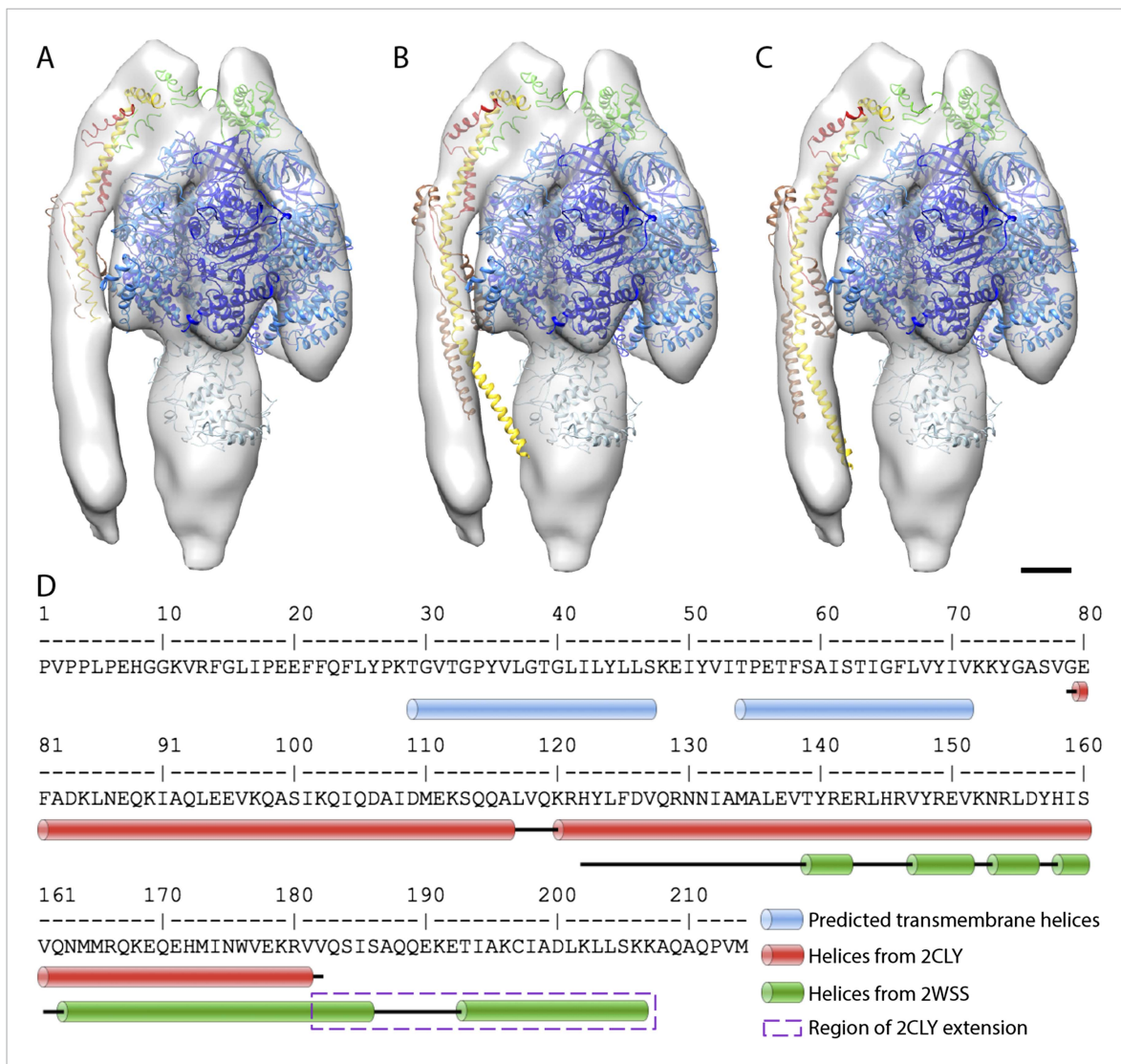


Figure 4—figure supplement 1. Possible atomic models fitted to sub-tomogram average. **(A)** Sub-tomogram average fitted with the F₁/peripheral stalk complex (PDB entry: 2WSS). **(B)** as in **(A)** but peripheral stalk extended with the atomic model of the peripheral stalk fragment (PDB:2CLY). **(C)** as in **(B)** but the extended peripheral stalk sub-complex plus C-terminal domain of the OSCP subunit fitted to the average as a rigid-body subsequent to the fitting of the F₁-subcomplex plus N-terminal domain of the OSCP subunit from 2WSS. **(D)** Sequence of the peripheral stalk subunit *b* from bovine heart showing the position of the predicted trans-membrane helices (blue) and the known helices (red and green) determined by x-ray crystallography. The dashed purple box indicates the residues from PDB:2WSS by which the PDB:2CLY structure was extended for rigid-body fitting in **(C)**. Atomic model subunit colors: blue, α ; dark blue, β ; light blue, γ, δ, ϵ ; yellow, *b*; red, *F₆*; brown, *d*; green OSCP. Scale bar: 20 Å.

DOI: 10.7554/eLife.06119.012

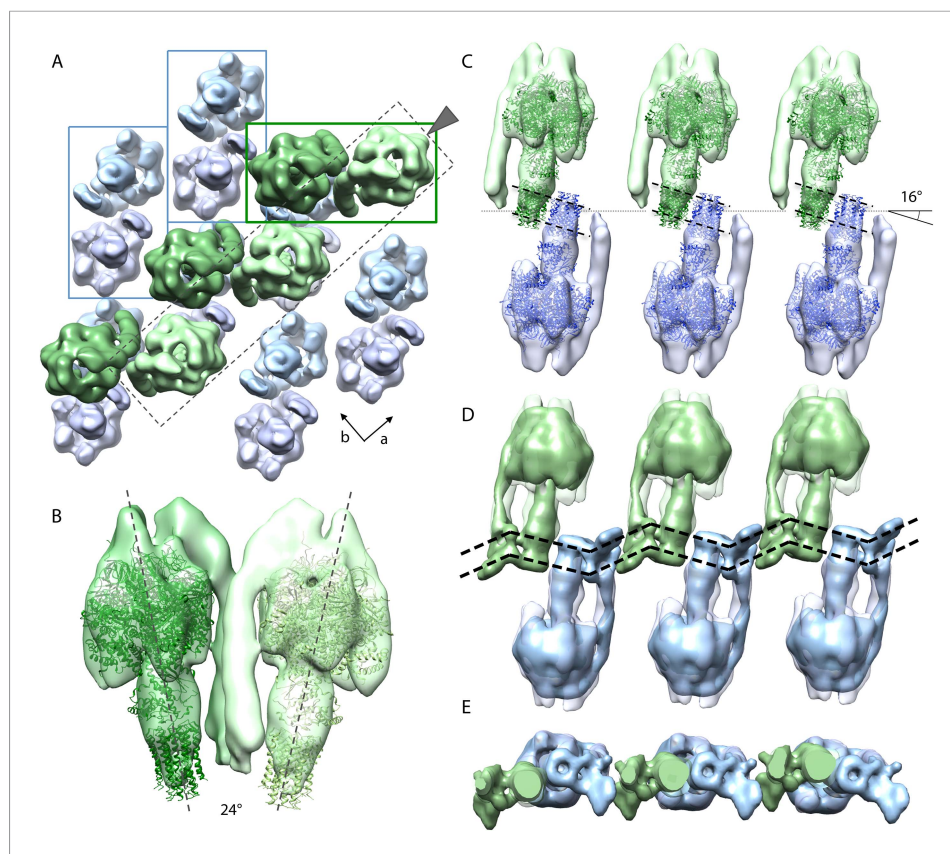


Figure 5. Packing of bovine F_1F_0 ATP synthase in the 2D crystal. **(A)** Top view of the 2D crystal lattice of bovine F_1F_0 ATP synthase. Rectangles indicate the position of ATP synthase pairs. Arrows indicate cell axes. **(B)** Side view of one pair. **(C)** Cross-section of the crystal lattice indicated by the dashed box and arrowhead in **(A)**. F_1F_0 ATP synthases of opposite orientation in the membrane are connected via close interaction of their rotor-rings. The rotor-ring pairs are oriented 16° relative to the crystal plane (single grey dashed line). **(D)** Cross-section as in **(C)** but with the single-particle EM map (Baker et al., 2012) fitted into the subtomogram averages. The arrangement of the monomeric complexes on the 2D crystal lattice results in a locally kinked lipid bilayer (bold dashed lines). **(E)** Top view of the cross-section in **(D)** clipped to remove the catalytic domains of the upper F_1F_0 ATP synthase layer.

DOI: [10.7554/eLife.06119.014](https://doi.org/10.7554/eLife.06119.014)

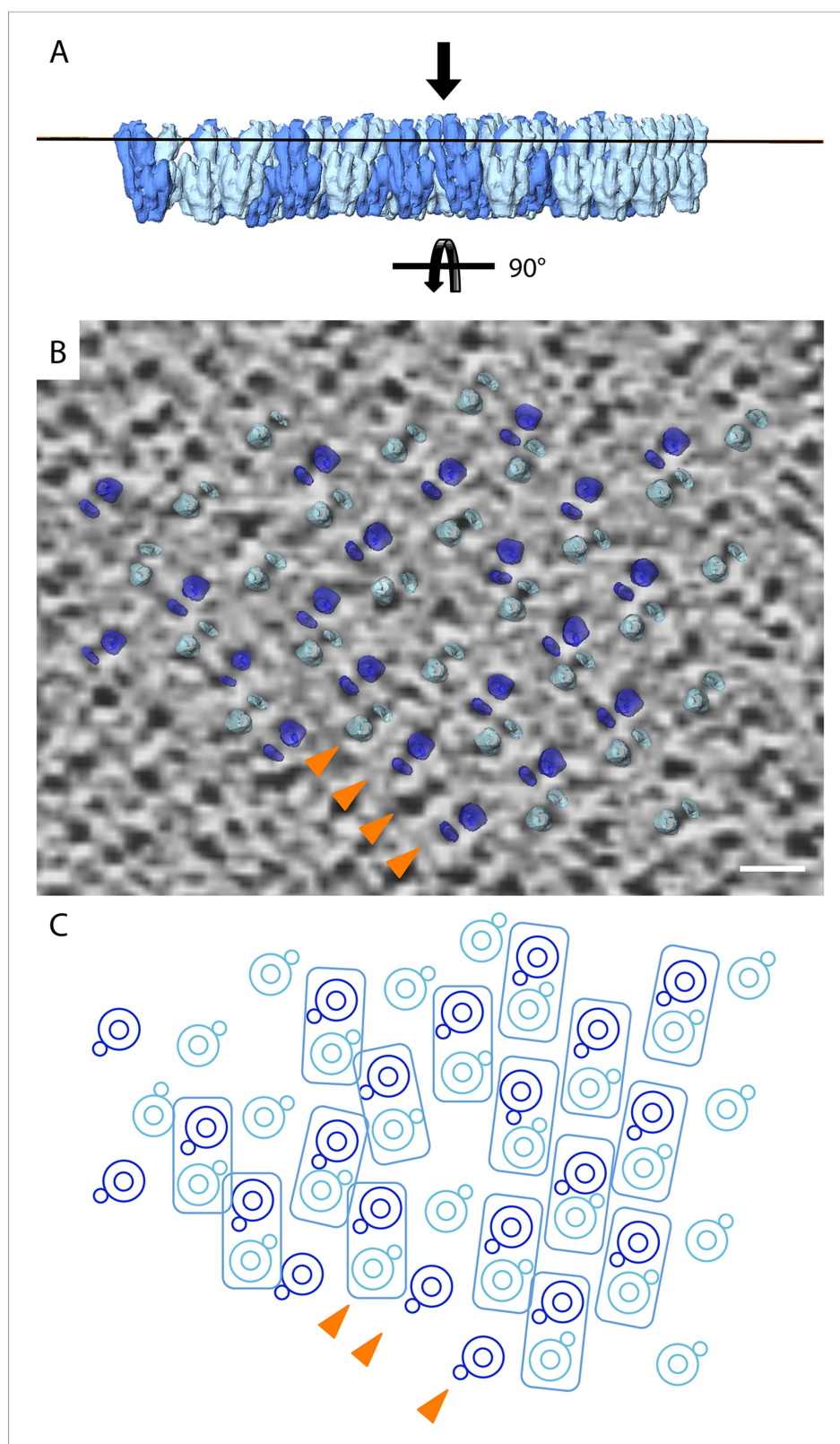


Figure 5—figure supplement 1. Lattice disorder. (A) Side view of subtomogram averages repositioned into the lower face of a 2D crystal. (B) Tomographic slice through a 2D crystal as indicated by line in (A) with a selection of repositioned sub-tomogram averages (transparent). The tomographic slice is viewed from the membrane (indicated Figure 5—figure supplement 1. continued on next page

Figure 5—figure supplement 1. Continued

by arrow in **A**). The repositioned subtomogram averages coincide with large and small circular densities, which correspond to the central and peripheral stalks, respectively (orange arrowheads). Scale bar: 10 nm. **(C)** Graphic representation of selected repositioned sub-tomogram averages in **(A)** highlighting the disorder in the crystal lattice. Small circles, peripheral stalk; double circle, F_1 -subcomplex + c-ring; rectangles indicate F_1F_o ATP synthase pairs. Arrowheads correspond to those shown in **(B)** and are included for orientation purposes.

DOI: [10.7554/eLife.06119.015](https://doi.org/10.7554/eLife.06119.015)

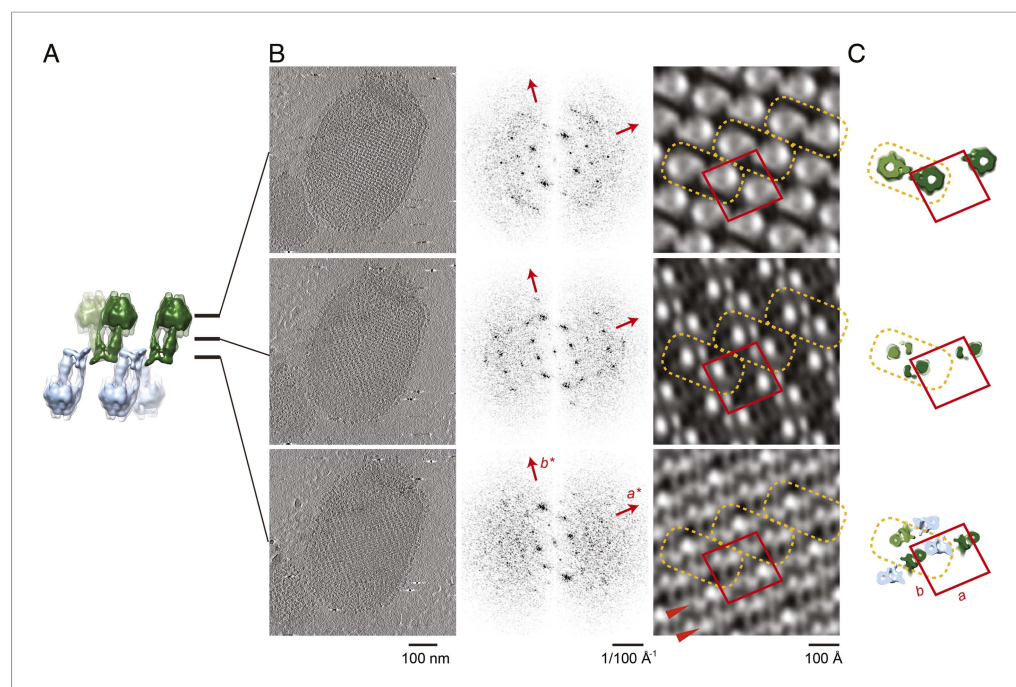


Figure 6. Projection maps of different z-slices in a 2D crystal of F_1F_o ATP synthases. **(A)** Side view of crystal packing from **Figure 4**. **(B)** Projection images (left) calculated from z-slices of the tomographic volume at z-height positions indicated by black bars in **(A)**, their Fourier transforms (centre) and projection maps (right). **(C)** z-slices through the crystal packing in **(A)** corresponding to the position of the projection maps shown in **(B)**. **(A–C)** Protein densities observed in the projection maps perfectly match the features shown in the corresponding z-slices of the crystal-packing model. Dashed orange outlines indicate a pair of F_1F_o ATP synthases, red boxes indicate the unit cell of the crystal with dimensions of $a = 179.1 \text{ \AA}$, $b = 171.4 \text{ \AA}$, $\gamma = 94.9^\circ$. Red arrowheads in the lower panel of **(B)** indicate lines of continuous protein density in the membrane plane.

DOI: [10.7554/eLife.06119.017](https://doi.org/10.7554/eLife.06119.017)

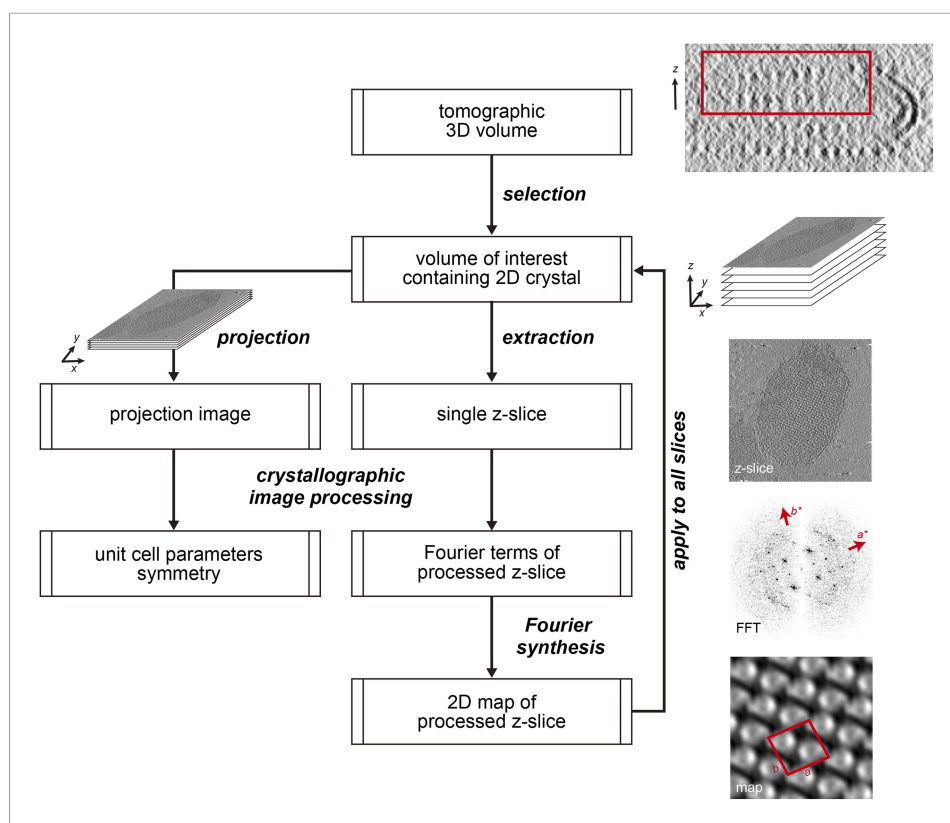


Figure 6—figure supplement 1. Flow chart of electron crystallographic image processing of a tomographic volume.

DOI: [10.7554/eLife.06119.018](https://doi.org/10.7554/eLife.06119.018)

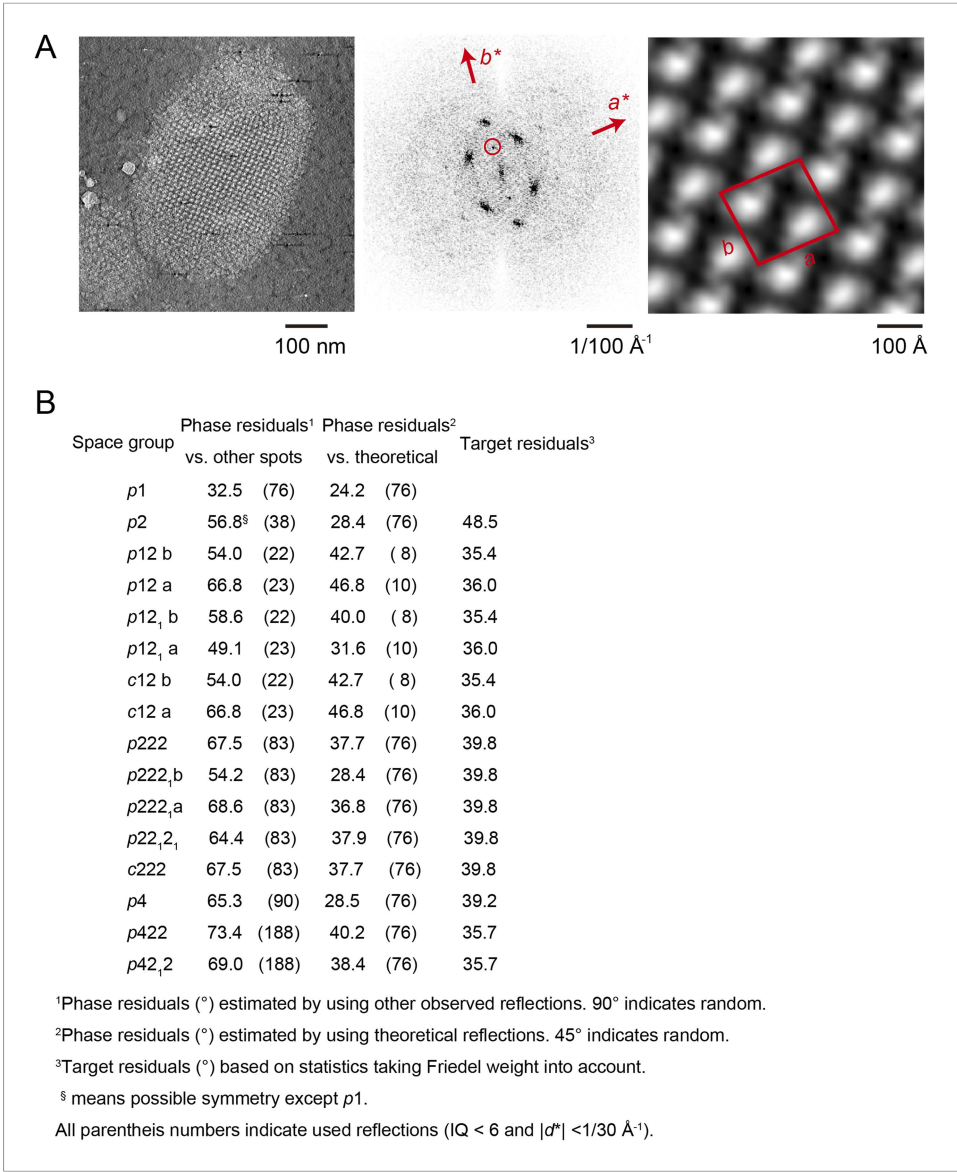


Figure 6—figure supplement 2. Unit cell parameters and crystal symmetry. **(A)** Projection images of tomographic z-slices containing the whole single-layered 2D crystal were processed to determine unit cell parameters and crystal symmetry. Image processing was performed using the MRC image processing programmes. **(A)** Projection image (left); Fourier transform (center); Fourier synthesis map (right). The red circle indicates the (0, 1) reflection. **(B)** The programme ALLSPACE did not indicate a clear plane-group symmetry for the 2D lattice.
[DOI: 10.7554/eLife.06119.019](https://doi.org/10.7554/eLife.06119.019)

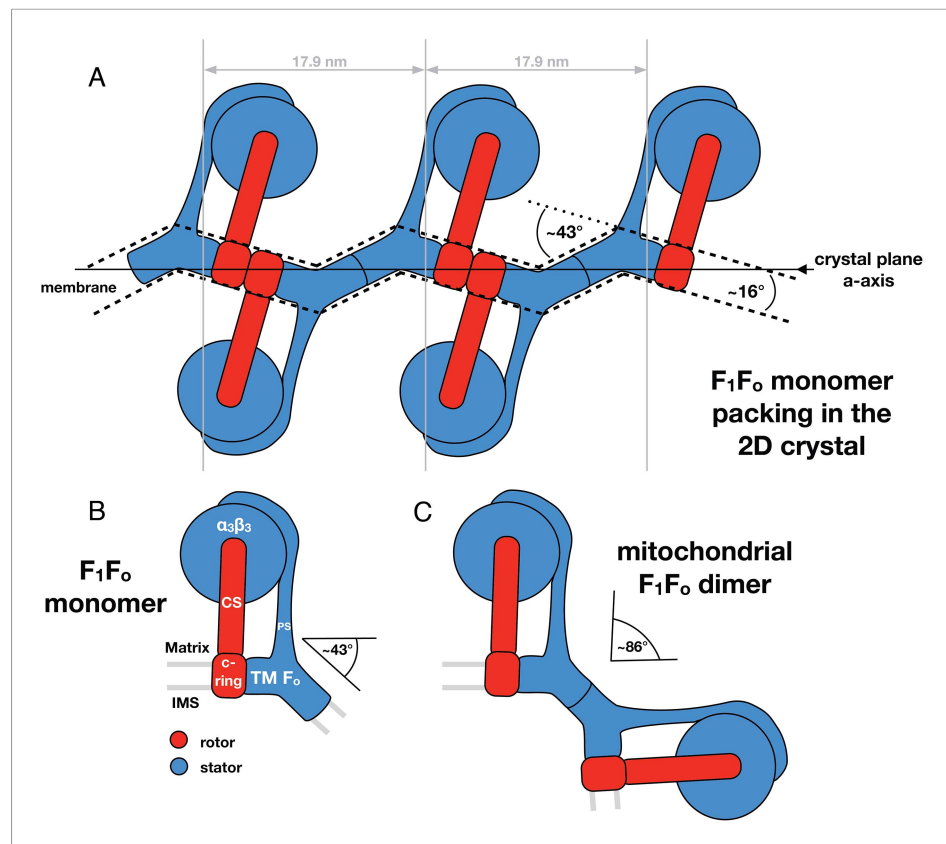


Figure 7. Monomeric mitochondrial F₁F₀ ATP synthase as the factor determining cristae membrane curvature. **(A)** Schematic diagram of bovine F₁F₀ ATP synthase in the 2D crystal lattice, with its transmembrane F₀ stator domain imposing a local 43° kink and a 16° inclination of the c-ring relative to the crystal plane. Blue, stator; red, rotor. **(B)** Schematic diagram of a single monomeric bovine F₁F₀ ATP synthase. CS: central stalk; PS: peripheral stalk; IMS: intermembrane space; TM F₀: transmembrane domain of F₀. **(C)** Association of two monomeric F₁F₀ complexes into a dimer results in an angle of 86°, as observed in ATP synthase dimers in mitochondrial cristae (Davies et al., 2012). DOI: [10.7554/eLife.06119.020](https://doi.org/10.7554/eLife.06119.020)